Solving momentum-space integral equations for quarkonium spectra with confining potentials. III. Bethe-Salpeter equation with spin

J. R. Spence and J. P. Vary
Department of Physics and Astronomy, Iowa State University, Ames, Iowa 50011
(Received 4 August 1992)

Singular integral equations for quarkonium ($q\bar{q}$) spectra are solved in momentum space for relativistic confinement plus Coulomb potentials including spin. The confinement potential in momentum space is defined using an analytical regularization scheme. Further manipulations give rise to integro-differential equations and we obtain analytical approximations for the remaining singular integrals. The procedure is tested with two different reductions of the Bethe-Salpeter equation. Using both scalar and scalar plus pseudoscalar confinement we obtain the spectra of charmonium, b-quarkonium, and the light mesons. We compare the results with experiment and with results obtained by other techniques. Eigenfunctions for selected eigenstates are presented. A good description of both the light and heavy mesons is then obtained with scalar linear confinement in the instantaneous approximation to the Bethe-Salpeter equation. This description is based upon the inclusion of a Breit term to approximate transverse gluon effects.

PACS number(s): 12.40.Aa, 12.40.Qq, 12.38.Lg

I. INTRODUCTION

There is considerable interest in developing a covariant description of the mass spectra and amplitudes of elementary particles based on QCD. Until such time as methods to directly solve QCD are perfected, the Bethe-Salpeter (BS) [1] integral equation with a phenomenological confining interaction should serve as an instructive model for the properties of the elementary particles. In this connection it is important to have stable and accurate methods to solve the BS equation in momentum space with nonlocal and singular kernels. We have adopted the quarkonium problem to illustrate a method for treating singular potentials in the BS equation with spin. We also present results for both the heavy and light mesons and compare with experiment and with some related theoretical investigations.

We begin by showing how confinement potentials for particles with spin may be defined in momentum space in such a manner that their partial wave decomposition is straightforward and yields a numerically tractable framework. A suitable basis for the numerical solution of integral equations containing such potentials is chosen, and the appropriate integrals are evaluated accurately and efficiently. We then apply this combination of techniques to evaluate the spectra of charmonium and b-quarkonium within the Blankenbecler-Sugar (BbS) reduction and within the instantaneous approximation (IA) to the BS equation. We use these frameworks to examine different Lorentz structures for confinement and to explore applications to the light mesons.

In an earlier work [2], which we refer to as I, confinement potentials in momentum-space integral equations for spinless particles were treated by introducing a cutoff. In a succeeding work [3], which we refer to as II, we introduced techniques to evaluate analytically the limit as the cutoff goes to zero. In the current work we employ the procedures of II together with standard results from the meson theory of nuclear forces to treat confinement potentials for particles with spin. As a result many of the techniques of relativistic nuclear physics developed to treat such potentials can be adapted in a straightforward manner. Thus the current work improves on the results of I and II in several ways and retains the advantage that general nonlocal potentials can be treated in addition to these singular potentials. The resulting methods are now quite general and applicable to a wide variety of problems beyond those treated here.

We have arranged the presentation in the following order. We begin in Sec. II with two reductions of the BS equation. In Sec. III we outline the single-boson-exchange and confinement contributions to the kernels, and Sec. IV gives the partial wave decomposition of the equations. Analytical methods for treating singularities are discussed in Sec. V, which are extensions to methods in II. Section VI and VII outline our spline methods for numerically solving the equations. We then present in Sec. VIII the results for charmonium and b-quarkonium using a simplified model neglecting the coupling of positive and negative frequency states. We extend the model by including this coupling plus approximate transverse gluon effect (the Breit term) in Sec. IX and present results for both the heavy and the light mesons. We conclude in Sec. X and discuss further applications of these models and methods.

II. EQUATIONS

Working in the center of momentum (CM) frame, we consider two three-dimensional reductions of the BS equation. The first reduction is an instantaneous approximation (IA), known as Salpeter's equation [4,5],

$$[E-E_a(\mathbf{q})-E_b(\mathbf{q})]\Lambda_a^+(\mathbf{q})\Lambda_b^+(\mathbf{q})\phi(\mathbf{q})=\Lambda_a^+(\mathbf{q})\Lambda_b^+(\mathbf{q})\int d^3q'G(\mathbf{q}-\mathbf{q}')[\Lambda_a^+(\mathbf{q}')\Lambda_b^+(\mathbf{q}')+\Lambda_b^-(\mathbf{q}')\Lambda_b^-(\mathbf{q}')]\phi(\mathbf{q}') \tag{1a}$$

and

$$[E+E_a(\mathbf{q})+E_b(\mathbf{q})]\Lambda_a^-(\mathbf{q})\Lambda_b^-(\mathbf{q})\phi(\mathbf{q})=-\Lambda_a^-(\mathbf{q})\Lambda^-(\mathbf{q})\int d^3q'G(\mathbf{q}-\mathbf{q}')[\Lambda_a^+(\mathbf{q}')\Lambda_b^+(\mathbf{q}')+\Lambda_a^-(\mathbf{q}')\Lambda_b^-(\mathbf{q}')]\phi(\mathbf{q}') . \tag{1b}$$

The $\Lambda^+(\mathbf{q})$ [$\Lambda^-(\mathbf{q})$] are projection operators that project positive [negative] energy free particle states and are defined by

$$\Lambda_a^{\pm}(q)=\frac{1}{2}\left[1\pm\frac{\boldsymbol{\alpha}_a\cdot\mathbf{q}+\beta_a m_a}{E_a(\mathbf{q})}\right] , \tag{2a}$$

$$\Lambda_b^{\pm}(q)=\frac{1}{2}\left[1\pm\frac{-\boldsymbol{\alpha}_b\cdot\mathbf{q}+\beta_b m_b}{E_b(\mathbf{q})}\right] , \tag{2b}$$

$$E_a(\mathbf{q})=+(m_a^2+\mathbf{q}^2)^{1/2} , \tag{2c}$$

$$E_b(\mathbf{q})=+(m_b^2+\mathbf{q}^2)^{1/2} . \tag{2d}$$

The kernel $G(\mathbf{q}-\mathbf{q}')$ represents the interaction between the particles, and denoting $\alpha^0=\beta$, the matrices α_a^μ and α_b^μ satisfy

$$\alpha_a^\mu\alpha_a^\nu+\alpha_a^\nu\alpha_a^\mu=2\delta^{\mu\nu} ,$$

$$\alpha_b^\mu\alpha_b^\nu+\alpha_b^\nu\alpha_b^\mu=2\delta^{\mu\nu} ,$$

$$\alpha_a^\mu\alpha_b^\nu-\alpha_b^\nu\alpha_a^\mu=0 ,$$

where $\mu,\nu=0,1,2,3$. There are two additional Salpeter equations, $\Lambda_a^+\Lambda_b^-\phi=0$ and $\Lambda_a^-\Lambda_b^+\phi=0$, which arise from making the instantaneous approximation and which have been implicitly included in our treatment.

The inclusion of coupling between positive and negative frequency states is particularly important for light mesons for which the energy gap between positive and negative frequency states is relatively small. It is also more important when considering interactions containing pseudoscalar terms because such terms couple positive and negative frequency states strongly. For these reasons inclusion of this coupling is crucial to the problem of attempting to determine the Lorentz structure of the confinement kernel when fitting both light and heavy meson spectra together [6]. However, since the inclusion of the coupling between positive and negative frequency states is not important for the examination of methods for solution to the BS equation, we defer them until Sec. IX and Eq. (1a) becomes

$$[E-E_a(\mathbf{q})-E_b(\mathbf{q})]\Lambda_a^+(\mathbf{q})\Lambda_b^+(\mathbf{q})\phi(\mathbf{q})=\Lambda_a^+(\mathbf{q})\Lambda_b^+(\mathbf{q})\int d^3q'G(\mathbf{q}-\mathbf{q}')\Lambda_a^+(\mathbf{q}')\Lambda_b^+(\mathbf{q}')\phi(\mathbf{q}') , \tag{3a}$$

and similarly by Eq. (1b).

A second three-dimensional reduction to the BS equation also explicitly treated here is the Blankenbecler-Sugar (BbS) [7] reduction which for the case $m_a=m_b=m$ has the form

$$\left[\varepsilon-\frac{\mathbf{q}^2}{m}\right]\Lambda_a^+(\mathbf{q})\Lambda_b^+(\mathbf{q})\bar{\phi}(\mathbf{q})=\Lambda_a^+(\mathbf{q})\Lambda_b^+(\mathbf{q})\int d^3q'\bar{G}(\mathbf{q}-\mathbf{q}')\Lambda_a^+(\mathbf{q}')\Lambda_b^+(\mathbf{q}')\bar{\phi}(\mathbf{q}') . \tag{3b}$$

Note that both the amplitude $\bar{\phi}(\mathbf{q}')$ and the kernel $\bar{G}(\mathbf{q}-\mathbf{q}')$ are different than for the IA.

III. KERNELS

In relativistic nuclear physics, systems containing two or three nucleons are often described by the use of some three-dimensional reduction of the BS equation or of a Faddeev equation. The nucleons interact by means of a sum of one-boson-exchange potentials (OBEP) [8,9]. These potentials are obtained by making the appropriate three-dimensional reductions of four-dimensional OBEP kernels of the form

$$G(q,q',\mu)=\frac{4\pi\gamma_0\otimes\gamma_0\Gamma_a\otimes\Gamma_b}{-(q-q')^2+\mu^2} , \tag{4}$$

where μ is the mass of the exchanged meson and

$$\Gamma_a\otimes\Gamma_b=1\otimes1,\gamma_5\otimes\gamma^5,\gamma_\mu\otimes\gamma^\mu,\ldots ,$$

$$q=\frac{q_a-q_b}{2},\quad q'=\frac{q_a'-q_b'}{2} ,$$

$$q_a=(q_{0a},\mathbf{q}_a),\quad q_b=(q_{0b},\mathbf{q}_b) .$$

Here the γ_μ denote the usual Dirac matrices.

For the IA such a three-dimensional reduction gives a potential which we denote by $V^{-1}(\mathbf{q},\mathbf{q}',\mu)$ and which is given by

$$V^{-1}(\mathbf{q},\mathbf{q}',\mu)=\frac{4\pi\gamma_0\otimes\gamma_0\Gamma_a\otimes\Gamma_b}{(\mathbf{q}-\mathbf{q}')^2+\mu^2} . \tag{5}$$

Since $\lim_{\mu\to0}(-\partial/\partial\mu)^{i+1}\exp(-\mu r)/r=r^i$, we define, as in I, the momentum-space kernel which corresponds to the coordinate-space kernel $V^i(r;\mu)=\gamma_0\otimes\gamma_0\Gamma_a\otimes\Gamma_b r^i e^{-\mu r}$ to be [8]

$$V^i(\mathbf{q},\mathbf{q}';\mu)\equiv\left[-\frac{\partial}{\partial\mu}\right]^{i+1}V^{-1}(\mathbf{q},\mathbf{q}';\mu) , \tag{6a}$$

with a class of singular potentials including confining

forms being given by

$$V^i(\mathbf{q},\mathbf{q}';0)\equiv\lim_{\mu\to 0}\left[-\frac{\partial}{\partial\mu}\right]^{i+1}V^{-1}(\mathbf{q},\mathbf{q}';\mu)\ . \tag{6b}$$

The limit $\mu\to 0$ is to be taken after integration over $\mathbf{q}'$.

Since the OBEP is simply the special case of (6a), with $i=-1$ many of the techniques and results developed for use with the OBEP may now be adapted with little change provided we know how to take the $\mu\to 0$ limit. Techniques to handle this limiting procedure were developed in I and II for the case without spin. Here we extend those methods to the general case with spin.

IV. PARTIAL WAVE DECOMPOSITION

A suitable basis for partial wave decomposition of the IA to the BS equation is the LSJ basis. With this basis eigenstates of the BS equation decouple into three [9–11] sets: singlet ($S=0$, $L=J$), uncoupled triplet ($S=1, L=J=1$), and coupled triplet ($S=1, L=J\pm 1$). Then, using the simplified notation $V(\mathbf{q},\mathbf{q}';\mu)\equiv V^{-1}(\mathbf{q},\mathbf{q}';\mu)$, the BS amplitude is the solution of

$$\langle JML'S|\psi(q)\rangle=\frac{1}{E-2E(q)}\sum_L\int dq'q'^2\langle JML'S|V(\mathbf{q},\mathbf{q}';\mu)|JMLS\rangle\langle JMLS|\psi(q')\rangle\ , \tag{7a}$$

where either $L=L'=J$ or $L=J\pm 1, L'=J\pm 1$.

We next give some standard results for the OBEP case in order to establish notation and then indicate how to adapt the results for our studies. Denoting $i^{(L'-L)}V^{LS}_{L'L}(q,q';\mu)=\langle JML'S|V(\mathbf{q},\mathbf{q}';\mu)|JMLS\rangle$ and $I^L\psi^J_L(q)=\langle JMLS|\psi(q)\rangle$, Eq. (7a) becomes

$$\psi^J_{L'}(q)=\frac{1}{E-2E(q)}\sum_L\int dq'q'^2V^{JS}_{L'L}(q,q';\mu)\psi^J_L(q')\ , \tag{7b}$$

with the sum over $L=J\pm 1$ for the coupled triplet case or over only the single term $L=J$ for the uncoupled triplet case and the single case. The quantities $V^{JS}_{L'L}$ can be written as linear combinations of quantities ${}^xV^J$; $x=0,1,12,34,55,66,a,b$, with the definitions singlet:

$$V^{J0}_{JJ}={}^0V^J\ ;$$

uncoupled triplet:

$$V^{J1}_{JJ}={}^1V^J\ ;$$

coupled triplet:

$$V^{J1}_{J-1,J-1}=\frac{1}{2J+1}[J\,{}^{12}V^J+(J+1)\,{}^{34}V^J+\sqrt{J(J+1)}\,{}^aV^J]\ ,$$

$$V^{J1}_{J+1,J+1}=\frac{1}{2J+1}[(J+1)\,{}^{12}V^J+J\,{}^{34}V^J-\sqrt{J(J+1)}\,{}^aV^J]\ ,$$

$$V^{J1}_{J-1,J+1}=\frac{1}{2J+1}[\sqrt{J(J+1)}\,{}^bV^J-J\,{}^{55}V^J+(J+1)\,{}^{66}V^J]\ ,$$

$$V^{J1}_{J+1,J-1}=\frac{1}{2J+1}[\sqrt{J(J+1)}\,{}^bV^J+(J+1)\,{}^{55}V^J-{}^{66}V^J]\ ,$$

$${}^aV^J\equiv{}^{55}V^J+{}^{66}V^J\ ,$$

$${}^bV^J\equiv{}^{12}V^J-{}^{34}V^J\ .$$

The details of the expressions for the ${}^xV^J$ differ with the Lorentz structure of the kernel and for other reductions of the BS equation. Since our procedure for generalizing the OBEP results to treat confinement is the same as in each case, we present only the scalar case with equal mass particles and within the IA.

For the scalar case define

$$F^{(0)}_S=-(E'E+m^2)\ ,$$

$$F^{(1)}_S=q'q\ ,$$

$$F^{(2)}_S=m(E'+E)\ ,$$

$$I^{(N)}_J\equiv\frac{Q^{(N)}_J(Z)}{q'q},\quad N=0,1,2,3\ ,$$

$$Q^{(0)}_J(Z)\equiv Q_J(Z)\ ,$$

$$Q^{(1)}_J\equiv ZQ_J(Z)-\delta_{J,0}\ ,$$

$$Q^{(2)}_J(Z)\equiv\frac{1}{J+1}[JZQ_J(Z)+Q_{J-1}(Z)]\ ,$$

$$Q^{(3)}_J(Z)\equiv\left[\frac{1}{J+1}\right]^{1/2}[ZQ_J(Z)-Q_{J-1}(Z)]\ ,$$

$$E=(q^2+m^2)^{1/2}\ ,$$

$$E'=(q'^2+m^2)^{1/2}\ ,$$

$$C_S=\frac{1}{2\pi EE'}\ ,$$

$$Z=\frac{q^2+q'^2+\mu^2}{2qq'}\ ,$$

where q (q') now denotes the magnitude of $\mathbf{q}$ ($\mathbf{q}'$) and $Q_J(Z)$ are the Legendre functions of the second type as defined below.

The explicit forms for the ${}^xV^J$'s for this case are then

$${}^0V^J_S=C_S[F^{(0)}_SI^{(0)}_J(Z)+F^{(1)}_SI^{(1)}_J(Z)]\ ,$$

$${}^1V^J_S=C_S[F^{(0)}_SI^{(0)}_J(Z)+F^{(1)}_SI^{(2)}_J(Z)]\ ,$$

$${}^{12}V^J_S=C_S[F^{(1)}_SI^{(0)}_J(Z)+F^{(0)}_SI^{(1)}_J(Z)]\ ,$$

$${}^{34}V^J_S=C_S[F^{(1)}_SI^{(0)}_J(Z)+F^{(0)}_SI^{(2)}_J(Z)]\ ,$$

$${}^{55}V^J_S=C_SF^{(2)}_SI^{(3)}_J(Z)\ ,$$

$${}^{66}V^J_S=C_SF^{(2)}_SI^{(3)}_J(Z)\ .$$

The results for the BbS reduction are similar [12].

V. TREATMENT OF SINGULARITIES

The Legendre functions of the second type, $Q_J(Z)$, are defined by

$$Q_0(Z)=\frac{1}{2}\ln\left[\frac{Z+1}{Z-1}\right],$$

$$Q_{J+1}(Z)=\left[\frac{2J+1}{J+1}\right]ZQ_J(Z)-\frac{J}{J+1}Q_{J-1}(Z)-\delta_{J,0}\,. \tag{8}$$

Because the $Q_J(Z)$ have logarithmic singularities when $q=q'$ and $\mu=0$, quantities of the form $\lim_{\mu\to 0}(-\partial/\partial\mu)^{i+1}Q_J(Z)$ require care in their interpretation [13]. As an example of our procedure for treating these singularities, consider the linear confinement case. If $K(q,q')$ is finite as $q\to 0$ and as $q\to\infty$, we may generalize the reasoning of II, starting with

$$-\lim_{\mu\to 0}\left[\frac{\partial}{\partial\mu}\right]^2 Q_0(Z)=P\frac{d}{dq'}\left[\frac{1}{q'+q}-\frac{1}{q'-q}\right],$$

and then integrating by parts twice and using the boundary conditions gives

$$\begin{aligned}\lim_{\mu\to 0}\left[\frac{\partial}{\partial\mu}\right]^2\int_0^\infty Q_0(z)K(q,q')\psi(q')dq' &= -(2/q)K(q,0)\psi(0)-P\int_0^\infty\left[\frac{1}{q'+q}-\frac{1}{q'-q}\right]\frac{\partial}{\partial q'}K(q,q')\psi(q')dq' \\ &= -(2/q)K(q,0)\psi(0)-\int_0^\infty\ln\left|\left|\frac{q'+q}{q'-q}\right|\right|\frac{\partial^2}{\partial q'^2}K(q,q')\psi(q')dq' \\ &= -(2/q)K(q,0)\psi(0)-\lim_{\mu\to 0}\int_0^\infty Q_0(Z)\frac{\partial^2}{\partial q'^2}K(q,q')\psi(q')dq'\,. \end{aligned} \tag{9}$$

Together with the relationship

$$\lim_{\mu\to 0}\left[\frac{\partial}{\partial\mu}\right]^2 ZQ_J(Z)=\lim_{\mu\to 0}\left[\frac{1}{qq'}Q_J(Z)+Z\frac{\partial}{\partial\mu^2}Q_J(Z)\right],$$

Eqs. (8) and (9) define the quantities $\lim_{\mu\to 0}(\partial/\partial\mu)^2Q_J(Z)$.

VI. SOLUTION OF THE EQUATIONS

As a specific case we consider the IA for equal mass particles interacting only through a linear confinement kernel. In the notation of Eq. (7b) we have

$$[E-2E(q)]\psi_L^{JS}(q)=\lim_{\mu\to 0}\sum_L\int_0^\infty dq'q'^2\left[\frac{\partial}{\partial\mu}\right]^2 V_{L'L}^{JS}(q,q';\mu)\psi_L^{JS}(q')\,.$$

To solve these equations the functions $\psi_L^{JS}(q)$ were assumed to have the convenient form $\psi_L^{JS}(q)=q^J\chi_L^{JS}(q)$. The functions $\chi_L^{JS}(q)$ were approximated as linear combinations of cubic B-splines with two continuous derivatives

$$\chi_L^{LS}(q)\approx\sum_{\mu=1}^{N}\beta_\mu^{JSL}B_\mu(q)\,,$$

and the singular quantities $\lim_{\mu\to 0}(\partial/\partial\mu)^2V_{L'L}^{JS}(q,q';\mu)$ were converted to integro-differential operators in the manner shown above. Then the coefficients β_μ^{JSL} were determined by a Galerkin [14] method chosen to yield symmetric matrices. The function $B_\mu(q)$ are then defined in terms of $N+4$ (distinct) knots $\{\tau_j\}$ by a recursion relation [15]. For $j>4$ these knots were chosen to be the images of the zeros $\{x_j\}$ of a Chebyshev polynomial

$$x_j=-\cos\left[\frac{2j-1}{2N\pi}\right]$$

under a mapping

$$\tau_{j+4}=\bar{q}\left[\frac{1+x_j}{1-x_j}\right]^{1/2}+\delta\,.$$

For $j\le 4$, $\tau_4=0$, and the remaining knots were chosen symmetrically so that

$$\tau_{4-j}=-\tau_{j+4},\quad j=1,2,3\,.$$

Satisfactory choices for $\bar{q}$ and δ, giving numerically stable results in all partial waves, were $\bar{q}=0.5$ GeV and $\delta=0.025$ GeV.

VII. EVALUATION OF INTEGRALS

In order to evaluate needed integrals of the form

$$\lim_{\mu\to 0}\left[-\frac{\partial}{\partial\mu}\right]^{i+1}\int_0^\infty dq'\frac{Q_J^{(N)}(Z)}{2qq'}F^{(M)}(q,q')B_\mu(q')\,, \tag{10}$$

the integrals

$$\lim_{\mu\to 0}\left[-\frac{\partial}{\partial\mu}\right]^{i+1}\int_{\tau_j}^{\tau_{j+1}}dq'\frac{Q_J^{(N)}(Z)}{2qq'}q'^{v}F^{(M)}(q,q')\ ,\qquad v=0,1,2,\ldots\ , \tag{11}$$

were evaluated with methods described below and the results substituted into the recursion relation defined the splines $B_\mu(q')$. To evaluate (11) each $F^{(M)}(q,q')$ was approximated on the interval $[\tau_j,\tau_{j+1}]$ by a cubic Hermite spline $\tilde{F}_j^{(M)}(q,q)$,

$$\tilde{F}_j^{(M)}(q,q')=\sum_{n=0}^{3}C_{nj}q'^{n}\ ,$$

satisfying both

$$\tilde{F}_j^{(M)}(q,q')=F^{(M)}(q,q')$$

and

$$\frac{\partial}{\partial q'}\tilde{F}_j^{(M)}(q,q')=\frac{\partial}{\partial q'}F^{(M)}(q,q')$$

at the end points $q'=\tau_j,\tau_{j+1}$. This yields the approximation

$$\lim_{\mu\to 0}\left[-\frac{\partial}{\partial\mu}\right]^{i+1}\int_{\tau_j}^{\tau_{j+1}}dq'\frac{Q_J^{(N)}(Z)}{2qq'}q'^{v}F^{(M)}(q,q')\approx\lim_{\mu\to 0}\left[-\frac{\partial}{\partial\mu}\right]^{i+1}\sum_{n=0}^{3}C_{nj}\int_{\tau_j}^{\tau_{j+1}}dq'\frac{Q_J^{(N)}(Z)}{2qq'}q'^{n+v}\ .$$

These integrals were evaluated analytically and the second (nonsingular) integration necessary for the Galerkin method was done numerically. An advantage of this procedure is that the quantities

$$I_1^{(m)}=\int_{\tau_j}^{\tau_{j+1}}dq'Q_0(Z)q'^{m},\quad m=0,1,2,\ldots\ ,$$

and

$$I_2^{(m)}=\int_{\tau_j}^{\tau_{j+1}}dq'q'^{m},\quad m=0,1,2,\ldots\ ,$$

need to be evaluated only once and the evaluation of integrals of the form (10) becomes a matter of forming linear combinations of them.

Evaluating the analytic expressions for the integrals $I_1^{(m)}$ and $I_2^{(m)}$ above require care to ensure numerical precision. Integrating by parts to set up recursion relations for $I_i^{(m+1)}$ in terms of $I_j^{(m)}$ yields expressions which are convenient to evaluate with precision. An exceptional case is when τ_j becomes large, where it is desirable to expand Q_0 in powers of $1/q'$ and keep a few leading terms.

Before introducing the complexity of coupling the positive and negative frequency results, we discuss results for this simpler model applied to the heavy quarkonium systems where it should be reasonably valid.

VIII. RESULTS AND DISCUSSION FOR THIS MODEL

Using a basis of 31 splines for each value of L, we solved for eigenenergies and eigenfunctions of the IA and BbS reductions of the BS equation with Coulomb plus confinement kernels,

$$\frac{-4\pi a\gamma_0\gamma_\mu\otimes\gamma_0\gamma_\mu}{-(q-q')^2}+4\pi b\lim_{\mu\to 0}\left[\frac{\partial}{\partial\mu}\right]^2\frac{\gamma_0\otimes\gamma_0\Gamma\otimes\Gamma}{-(q-q')^2+\mu^2}\ . \tag{12}$$

The results are presented in Table I. The calculation labeled IA(I) was done with $\Gamma\otimes\Gamma=1\otimes 1+\gamma_5\otimes\gamma^5$ (scalar plus pseudoscalar confinement) and the remainder labeled with IA(II) and BbS with $\Gamma\otimes\Gamma=1\otimes 1$ (pure scalar confinement). Results for related calculations [5], using a coordinate-space kernel corresponding to (12) with $\Gamma\otimes\Gamma=1\otimes 1$, are presented for comparison in the last two columns of Table I. These calculations are done with the same parameter set as in Ref. [5] to facilitate comparisons. That is, we use a charmed quark mass of 1.25 GeV, a bottom quark mass of 4.58 GeV, $a=0.25$, and $b=0.29$ GeV^2. No attempt to optimize or adjust these parameters has been made in this treatment, but we will fit the spectrum in Sec. IX below.

The calculations of Ref. [5] are most closely related to IA(II), but include coupling between positive and negative frequency states which we defer to the next section. However, since the role of these couplings is not expected to be large for the heavy mesons, we present the comparison here in order to calibrate our theoretical progress to this stage.

The results of Ref. [5] are obtained with a mixture of coordinate- and momentum-space methods, using harmonic oscillator eigenfunctions as a basis. There is a general consistency among the two calculations performed using the IA(I), IA(II), and also with the results of Ref. [5]. With the exception of the 0^- states and 2^+ states, the differences between the calculations are of the order of magnitude of the effect of our omission of coupling between negative and positive frequency states in the IA(II) calculations of this section. This effect is about 5–10 MeV in our IA(II) calculations and in the results cited in Ref. [5].

In the b-quarkonium spectrum we found, in addition to states corresponding to the observed 1^- states, which were primarily S states, two currently unobserved 1^- states having eigenenergies near 10100 and 10450 MeV. These states were almost pure D states, and their masses represent predictions of these calculations. We also present in Table I predictions for the lowest-lying $^1P_1$ state of b-quarkonium.

Comparing the BbS calculation with the IA calculation using the same kernel IA(II), we note that there is good

TABLE I. Quarkonium masses in MeV with kernels as given in text. The quantity $M_{\text{calc}} - M_{\text{expt}} \equiv \Delta$ is quoted for each set of theoretical results. The spectroscopic notation quoted for coupled states is that of the leading component in our calculations.

Meson	J^P	$^{2S+1}L_J$	M_{expt}	IA(I) M_{calc}	Δ	IA(II) M_{calc}	Δ	BbS M_{calc}	Δ	Ref. [5] M_{calc}	Δ
η_c	0^-	$^1S_0$	2979	3003	+24	3049	+70	3064	+85	2966	−13
J/ψ	1^-	$^3S_1$	3097	3117	+20	3105	+8	3145	+48	3095	−2
χ_0	0^+	$^3P_0$	3415	3468	+53	3437	+22	3555	+140	3434	+19
χ_1	1^+	$^3P_1$	3511	3460	−51	3462	−49	3591	+80	3475	−36
η_c	1^+	$^1P_1$	3526	3430	−96	3452	−74	3613	+87		
χ_2	2^+	$^3P_2$	3556	3536	−20	3528	−28	3673	+117	3447	−109
η_c	0^-	$^1S_0$	3590	3628	+38	3651	+61	3782	+192	3622	+32
ψ	1^-	$^3S_1$	3686	3694	+8	3691	+5	3842	+156	3682	−4
ψ	1^-	$^3D_1$	3770	3749	−21	3741	−29	3953	+183	3735	−35
ψ	1^-	$^3S_1$	4040	4093	+53	4094	+54	4371	+331	4085	+45
ψ	1^-	$^3D_1$	4159	4130	−29	4127	−32	4449	+290	4119	−40
ψ	1^-	$^3D_1$	4415	4411	−4	4414	−1	4820	+405	4405	−10
Υ	1^-	$^3S_1$	9460	9480	+20	9480	+20	9476	+16	9471	+11
Υ	0^+	$^3P_0$	9860	9826	−34	9825	−35	9836	−24	9822	−38
Υ	1^+	$^3P_1$	9892	9838	−53	9842	−50	9854	−38	9837	−55
Υ	1^+	$^1P_1$		9837		9841		9867			
Υ	2^+	$^3P_2$	9913	9909	−4	9907	−6	9926	+13	9843	−70
Υ	1^-	$^3S_1$	10023	10001	−22	10004	−19	10016	−7	9997	−26
Υ	1^-	$^3D_1$		10097		10099		10126			
Υ	0^+	$^3P_0$	10232	10227	−5	10229	−3	10255	+23	10225	−7
Υ	1^+	$^3P_1$	10255	10238	−17	10244	−11	10273	+18	10237	−18
Υ	2^+	$^3P_2$	10268	10300	+32	10299	+31	10328	+60	10244	−24
Υ	1^-	$^3S_1$	10355	10379	+24	10384	+29	10416	+61	10376	+21
Υ	1^-	$^3D_1$		10443		10448		10492			
Υ	1^-	$^3S_1$	10580	10694	+114	10701	+121	10756	+176	10693	+113

agreement for the eigenenergies of b-quarkonium. However, in the charmonium case where the quark mass is lighter, the agreement between IA(II) and BbS rapidly deteriorates with increasing charmonium mass. For this case of parameters the IA(I) and IA(II) provide a better phenomenological description of the quarkonium spectra than does the BbS. Both IA(I) and IA(II) also provide descriptions comparable to that provided in Ref. [5]. The rms deviations between calculations and experiment for charmonium are 42 MeV, 44 MeV, and 42 MeV for IA(II), IA(II), and Ref. [5], respectively. The rms deviations for b-quarkonium are 44 MeV, 46 MeV, and 49 MeV for IA(II), IA(II), and Ref. [5], respectively.

The differences in Table I between the IA results and the BbS results appeared to be due to the difference between the IA and BbS confinement kernels. This was determined by substituting the BbS kernel into the IA calculations and observing that the IA results with BbS kernel were considerably closer to the BbS results.

The derivations between the BbS results and experiment are large and tending in a single direction especially for charmonium. This suggests that the BbS results could be dramatically improved by adjusting the parameters of the model. A more detailed investigation of this issue and comparisons with additional reductions to the BS equation is in progress [6]. Our main purpose here is to outline our methods and obtain reasonable spectra with at least one reduction and one choice of confinement.

In Fig. 1 we give the radial dependence of the IA(II) eigenfunction for the first 0^- state of charmonium and in Fig. 2 that of the second 0^- state. Likewise, in Fig. 3 we give both the S and D components of the first 1^- state of charmonium and in Fig. 4 those of the third 1^- state. These eigenfunctions ϕ are normalized such that $\int_0^\infty \phi^2(q) q^2 dq = 1$. Figure 4 demonstrates well that L is not a good quantum number for this problem. It is also worth commenting again that the calculated 1^- state, shown in Fig. 4, is primarily a D state situated among other 1^- states which are primarily S states.

Noting that the x axis for these figures in units of

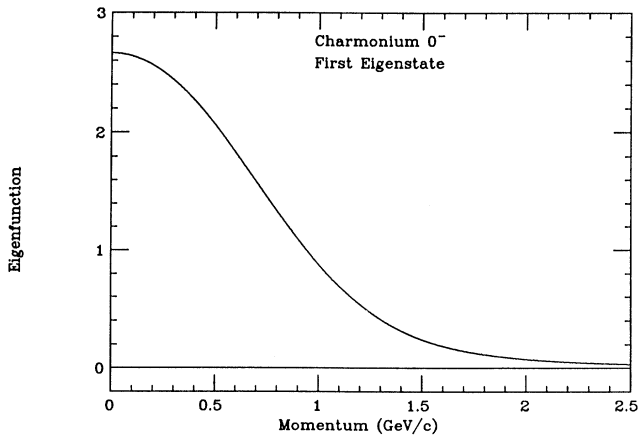

FIG. 1. Wave function for lowest 0^- eigenstate of charmonium calculated within IA(II) as a function of the magnitude of the quark three-momentum.

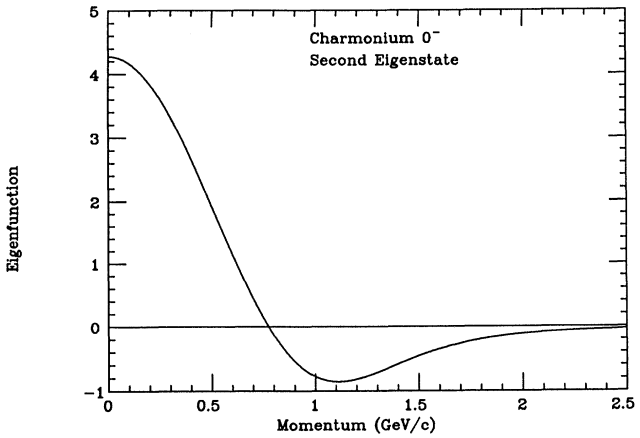

FIG. 2. Wave function for second 0^- eigenstate of charmonium calculated within IA(II) as a function of the magnitude of the quark three-momentum.

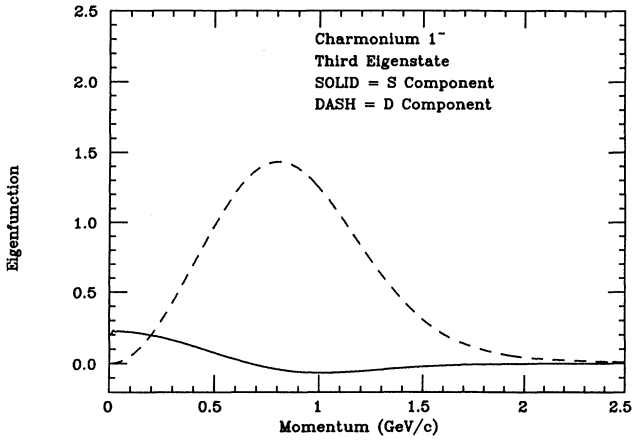

FIG. 4. Wave function for third 1^- eigenstate of charmonium calculated within IA(II) as a function of the magnitude of the quark three-momentum.

GeV/c and that we have taken the charmed quark mass to be 1.25 GeV, the relativistic nature of the problem is apparent. The relativistic nature of the problem is also apparent when comparing the eigenenergies in column IA(I) of Table I, for scalar plus pseudoscalar confinement, with those in columns IA(II), and those in BbS with scalar confinement. In the nonrelativistic limit these would all be equal, as is much the case with the behavior b-quarkonium systems. However, in the case of charmonium, the differences are already significant.

Comparing IA(I) and IA(II) we see the relativistic effects are apparently largest in the more tightly bound charmonium states. This is especially true of the 0^- states. On the other hand, comparing IA(I) and BbS shows that the relativistic effects can be large in the more highly excited charmonium states. Thus, we conclude that the relativistic effects may be significant and their precise values dependent on the BS reduction chosen for a *fixed* set of parameters.

Another agreement for the relativistic nature of charmonium is given in Table II where we present expectation values for a nonrelativistic velocity operator $V_{NR}=q/m$ and a corresponding relativistic expression $V_{\rm rel}=q/E(q)$ both calculated within IA(II). From the fact that the values presented are all larger than 0.48, we conclude that the motion of the constituents in this model is substantially relativistic. We therefore expect that the calculation of additional observables could readily yield results at variance with corresponding results from nonrelativistic models.

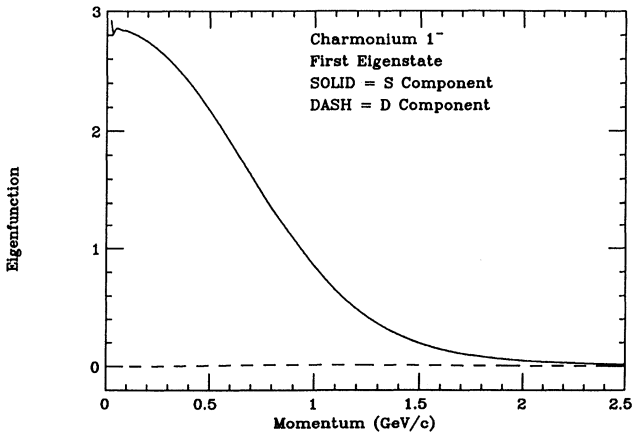

FIG. 3. Wave function for lowest 1^- eigenstate of charmonium calculated within IA(II) as a function of the magnitude of the quark three-momentum.

IX. EXTENDING THE MODEL TO THE LIGHT MESONS

In developing a general and relativistic QCD inspired model for the mesons, we find two further generalizations of the preceding treatment to be required in order for it to be applicable to the light mesons.

The first is to generalize previous methods for solving the BS equation in momentum space to include the coupling of positive and negative frequency states. The reason for this, as noted above, is that the effects of the mixing of positive and negative frequency components become very large for the lighter mesons. Hence, for an attempt to describe both the light mesons and the heavy mesons with the same equation and the same interaction, inclusion of such coupling is crucial. Furthermore, even

TABLE II. Expectation values of relativistic and nonrelativistic free particle velocity operators for some eigenstates of charmonium calculated with IA(II).

J^P	$M_{\rm expt}$	$V_{\rm NR}$	$V_{\rm rel}$
0^-	2979	0.6278	0.5005
0^-	3590	0.7328	0.5305
1^-	3097	0.5829	0.4898
1^-	3685	0.7174	0.5306
1^-	3770	0.7903	0.6054
1^-	4030	0.8394	0.5864
1^-	4160	0.8813	0.6261
1^-	4415	0.9372	0.6229

in the case of the heavy mesons we found, as discussed further below, that agreement with experimental spectra strongly constrains the Lorentz structure of the confinement kernel when this mixing is included.

The second generalization we found necessary for the treatment of the light mesons is the inclusion of a Breit term for one-gluon exchange. The Breit term represents certain transverse gluon effects, and we defer its discussion to the subsection on the light mesons.

A. Equations and methods for their solution

We continue to work in the center of momentum frame but, now, only with the instantaneous approximation to the BS equation [4]. At first sight the inclusion of the coupling between positive and negative frequency states would seem to offer no difficulty. The methods of the previous sections can be used to convert the IA with coupling between positive and negative frequency states into a matrix equation. When this is done the BS(IA) equation may be written as a matrix equation of the form

$$\begin{bmatrix} R & T \\ -T & -R \end{bmatrix} \begin{bmatrix} X_1 \\ X_2 \end{bmatrix} = E \begin{bmatrix} b & 0 \\ 0 & b \end{bmatrix} \begin{bmatrix} X_1 \\ X_2 \end{bmatrix} . \tag{13}$$

A major difficulty arises from the fact that the matrix

$$\begin{bmatrix} R & T \\ -T & -R \end{bmatrix}$$

is non-Hermitian and has trace equal to zero. These facts make direct approaches to the generalized eigenvalue problem of Eq. (13) numerically unstable. We find a satisfactory solution by starting with the generalized eigenvalue problem for the square of the energy. Writing Eq. (13) as

$$Ax = EBx ,$$

the equation for the square of the energy is

$$E^2 Bx = AB^{-1}Ax .$$

The roots of these equations for E^2 come in pairs which are all positive for the heavy mesons. These represent pairs of eigenvalues (positive and negative) of E, which correspond to positive and negative frequency solutions of the original equations. For lighter mesons, some pairs of roots of E^2 are negative, corresponding to pairs of purely imaginary eigenvalues for the energy. However, these imaginary roots appear far from the real roots of interest in the complex plane when we choose the spline basis as described in the preceding sections. Following an earlier work [5], we simply discard these imaginary roots. Presumably, these spurious solutions would be absent in a more complete treatment of the meson spectra.

B. Lorentz structure of the confinement kernel

Using a basis of 62 splines for each value of the L, we solved for eigenenergies of the IA reduction of the BS equation with Coulomb plus confinement kernels,

$$\frac{-4\pi a \gamma_0\gamma_\mu \otimes \gamma_0\gamma_\mu}{-(q-q')^2} + 4\pi b \lim_{\mu\to 0} \left[\frac{\partial}{\partial\mu} \right]^2 \frac{\gamma_0 \otimes \gamma_0 \Gamma \otimes \Gamma}{-(q-q')^2+\mu^2} . \tag{14}$$

The results are presented in Table III. The calculation labeled IA(I) was done with $\Gamma\otimes\Gamma = 1\otimes 1 + \gamma_5\otimes\gamma^5$, that labeled IA(II) with $\Gamma\otimes\Gamma = 1\otimes 1$, IA(III) with $\Gamma\otimes\Gamma = 1\otimes 1 - \gamma_5\otimes\gamma^5$, and IA(IV) was done with $\Gamma\otimes\Gamma = 1\otimes 1 + \gamma_\mu\otimes\gamma^\mu$. Thus, as in the previous sections, IA(I) corresponds to scalar plus pseudoscalar and IA(II) to pure scalar confinement. The case IA(III) is scalar minus pseudoscalar, and IA(IV) is composed of equal parts scalar and vector. We note here that our usage of the term "vector" is different from Refs. [16] and [17].

The values of the parameters a, b of Eq. (14) and the charmed and bottom quark masses were determined for each case separately by a least squares fit to the first six 1^- states of charmonium, the first three observed 1^- states of b-quarkonium, and the first two 0^- states of charmonium. Our procedure is to use these states to determine a set of parameters for each choice of Lorentz structure of the confinement kernel and then to observe how well each of the corresponding spectra agrees with experiment. As before, in the b-quarkonium spectrum we found, in addition to states corresponding to the observed 1^- states, two unobserved 1^- states having eigenenergies near 10100 and 10450 MeV in our calculations. We again give their eigenenergies as a prediction of these calculations. We also give the predictions for the lowest-lying $^1P_1$ state of b-quarkonium. For each Lorentz form of confinement, we give, in Table IV, the parameters for these fits, and the root mean square deviations between theory and experiment for all states shown in Table III.

Inspecting Tables III and IV, we conclude that IA(II), the pure scalar case, gives the best fit. Testing in this way, we conclude that if confinement is to be described as in Eq. (14), the Lorentz structure of the confinement kernel is largely or completely scalar. Put briefly, addition of a substantial vector or pseudoscalar portion to the confinement kernel shifts the relative spacings of the eigenstates so as to reduce the quality of the fit to the heavy meson spectra from those shown in previous sections. We can see that the origin of this deterioration in the quality of the fit is due to the coupling of positive and negative frequency states. This is illustrated by contrasting the quality of the fit of IA(I) in Table I with that of IA(I) in Table III where this coupling raises the overall rms deviation in the fit from 43 to 225 MeV for the scalar plus pseudoscalar confinement. On the other hand, for pure scalar confinement [IA(II)], the coupling of positive and negative frequency states results in a slight lowering of the overall rms deviation of the fit from 45 to 43 MeV. By way of further comparison we note that in Table III the IA(II) rms deviations from experiment are 34 MeV for charmonium and 52 MeV for b-quarkonium.

We note that in the calculations of the previous sections, in which this coupling of positive and negative frequency states were ignored, addition of a pseudoscalar term to the confinement kernel actually produced a slightly improved description. Because a pronounced

TABLE III. Quarkonium masses in MeV with kernels as given in text. The quantity $M_{\text{calc}}-M_{\text{expt}}\equiv\Delta$ is quoted for each set of theoretical results. The spectroscopic notation quoted for coupled states is that of the leading component in our calculations.

Meson	J^P	$^{2S+1}L_J$	M_{expt}	IA(I) M_{calc}	Δ	IA(II) M_{calc}	Δ	IA(III) M_{calc}	Δ	IA(IV) M_{calc}	Δ
η_c	0^-	$^1S_0$	2979	3187	+108	2969	−10	3003	+24	3070	+91
J/ψ	1^-	$^3S_1$	3097	3147	+50	3103	+6	3154	+57	3060	−37
χ_0	0^+	$^3P_0$	3415	3890	+475	3421	+6	3574	+159	3250	−165
χ_1	1^+	$^3P_1$	3511	3290	−214	3471	−40	3398	−113	3555	+44
η_c	1^+	$^1P_1$	3526	3672	+146	3461	−65	3565	+39	3178	−348
χ_2	2^+	$^3P_2$	3556	3271	−285	3535	+21	3177	−379	3597	+41
η_c	0^-	$^1S_0$	3590	3490	−100	3631	+41	3865	+273	3347	−243
ψ	1^-	$^3S_1$	3686	3551	−135	3689	+3	3468	−218	3631	−55
ψ	1^-	$^3D_1$	3770	3714	−56	3744	−26	3756	−14	3749	−21
ψ	1^-	$^3S_1$	4040	4016	−24	4080	+40	3999	−41	4078	+38
ψ	1^-	$^3D_1$	4159	4049	−110	4114	−45	4106	−53	4178	+19
ψ	1^-	$^3D_1$	4415	4128	−287	4377	−38	4134	−281	4459	+44
Υ	1^-	$^3S_1$	9460	9482	+22	9457	−3	9371	−89	9501	+41
Υ	0^+	$^3P_0$	9860	9806	−54	9815	−45	9789	−71	10039	+179
Υ	1^+	$^3P_1$	9892	9823	−69	9834	−58	9832	−60	9920	+28
Υ	1^+	$^1P_1$		9822		9824		9763		9589	
Υ	2^+	$^3P_2$	9913	9879	−34	9907	−6	9919	+6	10008	+95
Υ	1^-	$^3S_1$	10023	9993	−30	9995	−28	9981	−42	10037	+14
Υ	1^-	$^3D_1$		10077		10098		10102		10178	
Υ	0^+	$^3P_0$	10232	10214	−18	10245	+13	10208	−24	10470	+238
Υ	1^+	$^3P_1$	10255	10223	−32	10243	−12	10259	+4	10294	+39
Υ	2^+	$^3P_2$	10268	10144	−124	10197	−71	10235	+32	10297	+19
Υ	1^-	$^3S_1$	10355	10368	+13	10381	+26	10385	+30	10398	+43
Υ	1^-	$^3D_1$		10442		10450		10470		10498	
Υ	1^-	$^3S_1$	10580	10679	+102	10702	+122	10709	+129	10696	+116

deterioration in the quality of an actual fit is now observed with the addition of a substantial vector or pseudoscalar portion to the confinement kernel, this large effect may not be evident in the lowest-order nonrelativistic reduction of the Bethe-Salpeter equation (which does not account for the coupling of positive and negative frequency states).

C. Light mesons

The second step we found necessary for an accurate treatment of the entire meson spectrum with a single set of parameters was the inclusion of the Breit term. This term in the IA for the BS equation may be derived in a gauge invariant manner by expanding the quantity $1/[-(q-q')^2]$, in the gluon (or photon) propagator, in powers of $(q_0-q_0')^2$, obtaining

$$\frac{1}{-(q-q')^2}\simeq\frac{1}{(\mathbf{q}-\mathbf{q}')^2}+\frac{(q_0-q_0')^2}{(\mathbf{q}-\mathbf{q}')^4}\ . \tag{15}$$

The first term is the standard instantaneous Coulomb interaction, and the second term is a correction term describing the effects of transverse photons or gluons. Using the on shell free particle Dirac equations for the quarks, the second term in Eq. (15), the Breit term, may be written

$$V_{\text{Br}}=\frac{-4\pi a\,\boldsymbol{\alpha}_a\cdot(\mathbf{q}-\mathbf{q}')\otimes\boldsymbol{\alpha}_b\cdot(\mathbf{q}-\mathbf{q}')}{(\mathbf{q}-\mathbf{q}')^4}\ . \tag{16}$$

The Breit term, as given in Eq. (16), is inappropriate for incorporating directly into the BS kernel since it treats the mixing of positive and negative frequency states incorrectly. We invoke a standard remedy by inserting projection operators to eliminate such mixing by replacing

$$V_{\text{Br}}\rightarrow\Lambda_a^+\Lambda_b^+V_{\text{Br}}\Lambda_a^+\Lambda_b^++\Lambda_a^-\Lambda_b^-V_{\text{Br}}\Lambda_a^-\Lambda_b^-\ . \tag{17}$$

We note that by taking the four-dimensional generalization of the three-dimensional linear confinement potential (LCP) to be $1/[-(q-q')^4]$, it is possible to expand in powers of $(q_0-q_0')^2$ and obtain the corresponding Breit term for the LCP. We tested this possibility and found the effect of such a Breit term to be very small, and

TABLE IV. Parameters obtained by fitting the meson spectrum with kernels having the Lorentz structures described in the text. The masses of the charmed quark and of the bottom quark are labeled M_C and M_B, respectively. The parameters a and b govern the strength of the one-gluon-exchange and confining potentials, respectively. The total rms deviation between theory and experiment for the 21 states of Table III is quoted in the last column.

	M_C (GeV)	M_B (GeV)	a	b (GeV^2)	Total rms (MeV)
IA(I)	1.444	4.504	0.1604	0.3388	225
IA(II)	1.256	4.580	0.2666	0.2965	43
IA(III)	1.376	4.590	0.3581	0.3321	140
IA(IV)	1.287	4.718	0.3825	0.1134	120

TABLE V. Quarkonium masses in MeV for the IA(II) model with coupling between positive and negative frequency states and the Breit term included. As is customary we align the calculated states with the observed states according to their mass values for each spin parity starting from the lowest mass values. The asterisk on an experimental mass indicates a state employed in our fit. The values quoted from Ref. [17] are those using the Richardson potential [18]. See the caption to Table I.

Meson	J^P	$^{2S+1}L_J$	M_{expt}	IA(II) M_{calc}	Δ	Ref. [17] M_{calc}	Δ
η_c	0^-	$^1S_0$	2979*	2979	0	2996	+17
J/ψ	1^-	$^3S_1$	3097*	3097	0	3114	+17
χ_0	0^+	$^3P_0$	3415	3437	+22	3400	−15
χ_1	1^+	$^3P_1$	3511	3477	−34	3490	−21
η_c	1^+	$^1P_1$	3526	3422	−104		
χ_2	2^+	$^3P_2$	3556	3522	−34	3547	−9
η_c	0^-	$^1S_0$	3590*	3636	+46	3614	+24
ψ	1^-	$^3S_1$	3686*	3696	+10	3685	−1
ψ	1^-	$^3D_1$	3770*	3735	−35	3793	+23
ψ	1^-	$^3S_1$	4040*	4090	+50	4126	+86
ψ	1^-	$^3D_1$	4159*	4119	−40	4198	+39
ψ	1^-	$^3D_1$	4415*	4404	−11	4559	+144
Υ	1^-	$^3S_1$	9460*	9463	+3	9469	+9
Υ	0^+	$^3P_0$	9860	9809	−51	9849	−11
Υ	1^+	$^3P_1$	9892	9827	−65	9887	−5
Υ	1^+	$^1P_1$		9814			
Υ	2^+	$^3P_2$	9913	9889	−24	9915	+2
Υ	1^-	$^3S_1$	10023*	10077	+54	10021	−2
Υ	0^+	$^3P_0$	10232	10211	−21	10234	+2
Υ	1^+	$^3P_1$	10255	10227	−28	10258	+3
Υ	2^+	$^3P_2$	10268	10165	−103	10278	+10
Υ	1^-	$^3S_1$	10355*	10364	+9	10359	−10
Υ	1^-	$^3S_1$	10580	10679	+99	10647	+67

hence we chose not to include it here.

Using the IA(II) as discussed above and adding a Breit term of Eq. (17), the 11 selected states of the 0^- and 1^- spectra for charmonium and b-quarkonium were fitted as before to determine the charmed and bottom quark masses as well as the strengths of the one-gluon-exchange term and the pure scalar LCP term in the interaction. This resulted in a charmed quark mass of 1.248 GeV, a bottom quark mass of 4.538 GeV, $a=0.2427$, and $b=0.2867$ GeV^2. None of the light meson masses were used in determining the parameters in the interaction. To determine the masses for the u, d, and s quarks, we fitted the masses of the π, the ρ, and the ϕ. This resulted in a mass for the up and down quarks of 0.1540 and 0.2406 GeV for the strange quark mass.

For Coulomb and confinement potentials the combination of procedures outlined above satisfies the criteria of accuracy and stability in a small spline basis. Because one integration was done analytically, the amount of computer time was reasonable. The final version of the program, used to generate the results in Tables V–VII, which follow, took between 5 and 25 min of CPU time on

TABLE VI. Selection of lighter mass mesons formed from equal mass fermion pairs. See the captions to Tables I and V.

Meson	$q\bar{q}$	$^{2S+1}L_J$	M_{expt}	IA(II) M_{calc}	Δ	Ref. [17] M_{calc}	Δ
π	$u\bar{u}$	$^1S_0$	140*	144	+4	143	+3
ρ	$u\bar{u}$	$^3S_1$	768*	715	−53	629	−139
f_0	$s\bar{s}$	$^3P_0$	974	1260	+286	1231	+257
a_0	$u\bar{u}$	$^3P_0$	983	1085	+102	731	−252
ϕ	$s\bar{s}$	$^3S_1$	1019*	1022	+3	1063	+44
b_1	$u\bar{u}$	$^1P_1$	1232	893	−339	1195	−37
a_1	$u\bar{u}$	$^3P_1$	1260	997	−263	1222	−38
π	$u\bar{u}$	$^1S_0$	1300	1298	−2	1363	+63
a_2	$u\bar{u}$	$^3P_2$	1318	1191	−127	1367	+49
f_1	$s\bar{s}$	$^3P_1$	1426	1340	−86	1499	+73
f'_2	$s\bar{s}$	$^3P_2$	1525	1523	−2	1630	+105
π_2	$u\bar{u}$	$^1D_2$	1670	1527	−143	1774	+104
ϕ'	$s\bar{s}$	$^3S_1$	1680	1746	+66	1831	+151

TABLE VII. Selection of mesons formed from unequal mass fermion pairs. See the captions to Tables I and V.

Meson	$q\bar{q}$	$^{2S+1}L_J$	M_{expt}	IA(II) M_{calc}	IA(II) Δ	Ref. [17] M_{calc}	Ref. [17] Δ
K	$s\bar{u}$	$^1S_0$	496	496	0	485	−11
K^*	$s\bar{u}$	$^3S_1$	892	899	+7	839	−53
D	$c\bar{u}$	$^1S_0$	1865	1814	−51	1770	−95
D^*	$c\bar{u}$	$^3S_1$	2010	2147	+137	1918	−92
D_S	$c\bar{s}$	$^1S_0$	1969	1902	−67	1981	+12
D_S^*	$c\bar{s}$	$^3S_1$	2110	2281	+171	2119	+9
B	$b\bar{u}$	$^1S_0$	5279	5003	−276	5169	−110

a VAX8600 for each partial wave. Because the analytical evaluation of the singular first integration was reduced to forming linear combinations of certain fundamental integrals, the procedures described here are highly suited for vectorization. After some optimization and vectorization the program took between 1.4 and 20 sec on a Cray YMP, for each partial wave.

The new fit with the Breit term and the resulting additional states of the heavy mesons are given in Table V. For comparison we present results for the corresponding states from Crater and Van Alstine [17], who employed their two-body Dirac constraint dynamics approach to fit a larger set of heavy mesons masses. Our IA(II) results in Table V now have an overall rms deviation of 45 MeV from experiment compared with 42 MeV in Table III. The results of Ref. [17] in Table V have an overall 42 MeV rms deviation from experiment. Considering that our results and those of Ref. [17] arise from different fitting strategies, they may be viewed as roughly comparable descriptions of these data.

With the interactions now determined only by our fit to the heavy meson masses, we present our results for a set of lighter mesons in Tables VI and VII along with the corresponding results from Ref. [17]. Only three mesons from Tables VI and VII were used to determine our light quark masses. The majority of our masses in these tables constitute, in a sense, the predictions of our model.

The IA(II) results in Table VI have a 159 MeV rms deviation from experiment, while the corresponding quantity for the Ref. [17] results is 127 MeV. In Table VII the IA(II) results exhibit a 137 MeV rms deviation from experiment, while those of Ref. [17] have only a 68 MeV rms deviation from experiment. To aid in understanding the lower rms values from the results of Ref. [17], we note that all but one of the 20 masses in Tables VI and VII were utilized in their fit to determine the interaction parameters and the quark masses.

X. CONCLUSIONS AND OUTLOOK

In this paper we have presented two types of results: (1) methods for solving Bethe-Salpeter wave equations for two spin 1/2 fermions interacting via one-boson-exchange potentials plus linear confinement and (2) applications of those methods to develop a unified model for the light and heavy mesons which has success comparable with existing models. We obtain a relativistic description of the light and heavy meson spectra utilizing the instantaneous approximation (IA) to the Bethe-Salpeter (BS) equation. In so doing, we find that a scalar linear confinement and a Breit term to approximate transverse gluon effects work well together to produce a more reasonable fit. We imagine that our description of the meson masses can be further improved by increasing the number of light mesons involved in the fitting procedure and by adjusting the interaction terms to simultaneously fit light and heavy mesons. This takes us beyond the philosophy of the current endeavors but will be approached in the future [6].

The utility of these methods goes well beyond the applications we have demonstrated here and we will give some brief examples.

First we have adopted these methods in order to solve e^+-e^- scattering and have obtained resonances which could serve as an explanation of anomalous e^+-e^- coincidence peaks in heavy ion experiments [19]. The continuum problem with a one-photon-exchange kernel is much more difficult than the corresponding bound state problem because, in addition to having singularities in the kernel of the BS equation, one has singularities in the solution to the BS equation. An extension to the unequal mass case of e^--p scattering has been completed [20]. Second, given the efficiency of these methods for the relativistic two-fermion problem, it appears natural to extend them to the relativistic three-fermion problem. Third, finite element methods of the type described here generally converge much more rapidly than do low-lower finite difference methods. Thus the methods introduced here open an alternative avenue for addressing nonperturbative treatments of QCD which we are presently investigating.

ACKNOWLEDGMENTS

We are pleased to acknowledge discussions with B. C. Clark, R. J. Perry, and A. J. Sommerer. This work was supported in part by the National Science Foundation Grant Nos. PHY86-00702 and PHY87-19526, by the U.S. Department of Energy under Grant No. DE-FG02-87ER40371, Division of High Energy and Nuclear Physics, and by a grant of computer time from the Ohio Supercomputer Center. This research was also supported in part by the National Science Foundation under Grant No. PHY82-17853, supplemented by funds from the National Aeronautics and Space Administration.

[1] H. A. Bethe and E. E. Salpeter, Phys. Rev. **82**, 309 (1951); **84**, 1232 (1951).
[2] D. Eyre and J. P. Vary, Phys. Rev. D **34**, 3467 (1986), hereafter denoted as I.
[3] J. R. Spence and J. P. Vary, Phys. Rev. D **35**, 2191 (1987), hereafter denoted as II.
[4] E. E. Salpeter, Phys. Rev. **87**, 328 (1952).
[5] Chris Long, Phys. Rev. D **30**, 1970 (1984).
[6] A more extensive investigation involving additional reductions in the BS equation is under study and will be report-

ed elsewhere.
[7] R. Blankenbecler and R. Sugar, Phys. Rev. **142**, 1051 (1966).
[8] N. Niamai Singh, Y. K. Mathur, and A. N. Mitra, Few-Body Syst. **1**, 47 (1986).
[9] Joseph J. Kubis, Phys. Rev. D **6**, 547 (1972).
[10] K. Erkelenz, Phys. Rep. C **13**, 191 (1974).
[11] M. J. Zuilhof and J. A. Tjon, Phys. Rev. C **22**, 2369 (1980).
[12] R. Machleidt, K. Holinde, and Ch. Elster, Phys. Rep. **179**, 1 (1987).
[13] W. D. Heiss and G. M. Welke, J. Math. Phys. **27**, 936 (1986).
[14] K. E. Atkinson, *A Survey of Numerical Methods for the Solution of Fredholm Equations of the Second Kind* (SIAM, Philadelphia, 1976).
[15] C. DeBoor, *A Practical Guide to Splines* (Springer, Berlin, 1978).
[16] H. W. Carter and P. Van Alstine, Phys. Rev. Lett. **53**, 1527 (1984).
[17] H. W. Carter and P. Van Alstine, Phys. Rev. D **37**, 1982 (1988).
[18] J. Richardson, Phys. Lett. **82B**, 272 (1979).
[19] J. R. Spence and J. P. Vary, Phys. Lett. B **254**, 1 (1991).
[20] J. R. Spence and J. P. Vary, Phys. Lett. B **271**, 27 (1991).